

Miniaturized fluorescence detection chip for capillary electrophoresis immunoassay of agricultural herbicide atrazine

Kyeong-Sik Shin^{a,c}, Young-Hwan Kim^a, Jung-Ah Min^a, Seoung-Min Kwak^a,
Sang Kyung Kim^a, Eun Gyeong Yang^b, Jung-Ho Park^c, Byeong-Kwon Ju^d,
Tae-Song Kim^a, Ji Yoon Kang^{a,*}

^a *Microsystem Research Center, Korea Institute of Science and Technology, Seoul 136-791, Republic of Korea*

^b *Biomedical Research Center, Korea Institute of Science and Technology, Seoul 136-791, Republic of Korea*

^c *Department of Electronics Engineering, Korea University, Seoul 136-701, Republic of Korea*

^d *Department of Electrical Engineering, Korea University, Seoul 136-701, Republic of Korea*

Received 1 December 2005; received in revised form 27 May 2006; accepted 30 May 2006

Available online 17 June 2006

Abstract

This paper reports a miniaturized fluorescence detection chip for capillary electrophoresis immunoassay of atrazine, which effectively reduces the size of fluorescence detection system. The photodiode with fluorescence filter was embedded in PDMS (polydimethylsiloxane) microfluidic chip and was placed just below the microfluidic channel. This detection chip is only few mm thick without loss of fluorescence due to the proximity of photodiode and channel. To investigate the feasibility of in situ detection of agricultural herbicide, atrazine was detected using capillary electrophoresis immunoassay in microfluidic chip. Mixture of 570 nM fluorescence-labeled atrazine (Ag*) and 700 nM anti-atrazine antibody (Ab) was injected and separated in 25 mm long microfluidic channel. The separated peaks of Ab-Ag* immunocomplex and Ag* were detected by the miniaturized detector and the change of peak magnitude was also observed with the variation of Ab concentration. The result was verified with those of external PMT (photomultiplier tube) and commercial capillary electrophoresis system. Hence, we have demonstrated the feasibility of portable CE immunoassay of atrazine with on-chip fluorescence detector.

© 2006 Elsevier B.V. All rights reserved.

Keywords: Capillary electrophoresis (CE); Fluorescence detection chip; Microfluidic channel; Polydimethylsiloxane (PDMS); Photodiode; Atrazine

1. Introduction

Lab-on-a-chip has been developed into a flourishing area since the first report was published in 1990 by Manz et al. [1]. A room full of instruments can be incorporated into a compact chip achieving sample pretreatment, high-throughput analysis through parallel sample processing, electrophoretic or chromatographic separations. Among many applications of lab-on-a-chip, microchip capillary electrophoresis (CE) is considered as one of the successful areas and microfluidic chips for separation are already commercially available in the market. It shortens sample analysis time from minutes to seconds owing to the short length of the separation channel and the small size of the sample plug. Last but not the least is the significant

reduction in production cost because fabrication cost is low and typical microchip CE system only consumes nano-liter of analytes or reagents [2,3]. CE has since attracted much interest in other application areas, including pesticide-residue determination. Also, its capability to conduct analysis in a miniaturized format (microchip technology) is interesting for the routine analysis of samples containing hazardous pesticides. However, to realize the benefits of CE in the analysis of pesticide residues, we must overcome its inadequate detection sensitivity due to the small sample volumes typically injected. The sensitivity of CE can be enhanced by using a more sensitive detection method or introducing a sample-enrichment step before separation. The growing importance of CE in the field of pesticide-residue analysis is emphasized by the appearance of the first review article dealing with the different aspects of its environmental applications [4–7]. So far, however, most of these applications are restricted to the demonstrations performed by bulky commercial instruments.

* Corresponding author. Tel.: +82 2 958 6747.

E-mail address: jykang@kist.re.kr (J.Y. Kang).

Hence if CE equipment is miniaturized, it is suitable for portable diagnostic kit. Microchip for CE is small and cheap enough to be portable and disposable owing to the microfabrication. In addition microchip device offers further advantage in integrating on-line pre-column reactions and massive parallel analysis. However, optical detection systems for fluorescence in microchannel are still relatively large and expensive. The realization of the portable CE immunoassay devices requires small, portable and inexpensive fluorescence detection system.

Since the small volume in microfluidic channel results in the short path through samples for optical detection, highly sensitive detection is therefore a pre-requisite when performing analysis in microfluidic systems [8]. Fluorescence detection of microfluidic devices usually implements laser-induced fluorescence (LIF) with excellent sensitivity. However the large optics and detector is not appropriate for portable application. Hence the integration of sensitive photo-detection scheme in microfluidic chip is a major challenge in portable fluorescence detection. From the viewpoint of photo detector, the photomultiplier tube (PMT), photo-transistor (PT) and photodiode (PD) are considered as a photo-detector. PMT is usually used in commercial bulky systems and occasionally used for integrated fluidic channels [9]. Although photodiode is not as sensitive as PMT, it is easily integrated into microfluidic chip and silicon-based photodiode is inexpensive and easy to fabricate in microfabrication foundry. Hence, in many other reports, diode chips were used as photo detectors on silicon or glass substrates taking advantage of the small size and feasible fabrication process [10,11]. However, to achieve reasonable sensitivity with photodiode, integrated fluorescence detection chip needs the special design of optical path [12]. The design aims at the reduction of background noise from the light source and the enhancement of the collection efficiency of emission from the samples. Waveguide, optical fiber or microlens has been utilized to improve the signal to noise ratio despite additional design complexity. Although the complicated optical path can increase the efficiency, it either makes the size of system large or raises the cost of fabrication process. Since simple and smallest optical scheme is preferred for low cost solution, we selected simple fluorescence detection scheme to minimize the fabrication complexity. The fully packaged microchip with fluorescence detector consists of photodiode, interference filter and microfluidic channel. For higher sensitivity of fluorescence, the finger-type PIN photodiode was designed for separation channel and fabricated. The interference filter was deposited directly onto the photodiode to transmit fluorescence-emission and to block the background noise from excitation light. PDMS (polydimethylsiloxane) was used as an adhesive layer to assemble the PDMS microfluidic channel slab unit and silicon device unit composing one monolithic on-chip fluorescence detector. The PDMS-based bonding method was effective to minimize distance between the two units [13–16]. Hence, PDMS was used as channel layer or interlayer between the microfluidic channel on glass and the photodiode on silicon [17–22].

This paper describes the feasibility study of CE immunoassay using an integrated fluorescence detection system, implemented by a PIN photodiode and PDMS microfluidic chip. Fabricated

miniaturized fluorescence detection chip was applied to assay herbicide atrazine by microchip CE immunoassay.

2. Experimental

2.1. Design and fabrication of photodiode

PIN photodiode was fabricated on a silicon substrate and covered with interference optical filter that was directly deposited on the substrate. It allows the transmission of emitted fluorescence, and also blocks the background noise from excitation light. A PIN finger-type photodiode was designed for a lateral and shallow depletion region improving the collection efficiency. It was reported that the most visual spectrum range is absorbed within 1 μm depth of silicon from the oxide interface [23,24]. Therefore, we designed the junction depth as 150 nm in the p^+ region. The finger-type photodiode was adopted to use the side depletion region between the n^+ region and the p^+ region to reduce the parasitic resistance. The fabrication process of the designed photodiode was simulated by TSupremeTM and the depth at the maximum concentration in the p^+ region was calculated to be 80 nm thick. The PIN photodiode was fabricated on an n-type silicon substrate with the resistivity of 4 $\text{k}\Omega\text{ cm}$. Arsenic was implanted with the energy of 80 keV and the dose of $3 \times 10^{15}\text{ cm}^{-2}$ to form n^+ and p^+ regions, and boron was implanted with the energy of 30 keV and the dose of $5 \times 10^{15}\text{ cm}^{-2}$. After implantation, annealing step was carried out to activate the dopants. TEOS (tetraethoxysilane) silicon oxide was deposited as a passivation layer of 500 nm thickness. Optical interference filter of 2.3 μm thickness was directly deposited on the photodiode, which consists of 16-pairs of $\text{SiO}_2/\text{TiO}_2$ layer. Finally, for metal connection, contact hole was patterned, and chrome electrodes were formed by metallization process.

2.2. Fabrication of microfluidic chip and packaging of photodiode

PDMS (polydimethylsiloxane) chips are prepared by soft lithography with SU8 mold. The width and depth of microfluidic chip are about 70 and 12 μm , respectively. The microchip is 25 mm wide and 50 mm long with a four-way injection cross, 27 mm-long separation channel and 8 mm-long side channels. To bond a microchannel slab and a photodiode, the packaging process of a photodiode in PDMS was carried out as shown in Fig. 1A. The PDMS was spin-coated to form 20 μm thick film, which is a gap from channel to photodiode, on the PES (polyether sulfone) flexible substrate at 85 $^\circ\text{C}$ for 5 min. The PD was placed on the PDMS film with its face down and then liquid PDMS was poured on it to embed the photodiode in PDMS. PDMS was cured at room temperature overnight to avoid the mechanical stress to the photodiode. This procedure allowed the liquid PDMS to flow under the wire connected to the metal electrode. The photodiode-embedded PDMS slab was removed with ease from the flexible PES substrate by peeling-off process. We sealed the channel with photodiode-embedded PDMS slab by the process of oxygen plasma bonding, which could reduce the thermal stress and preserve the original geometry of

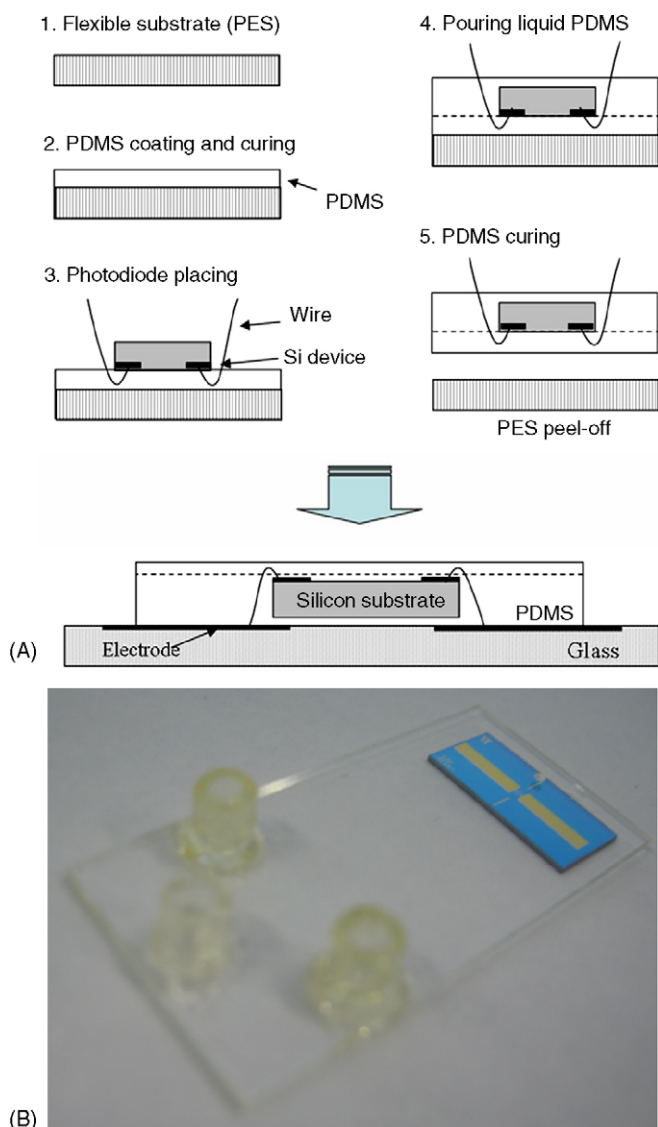


Fig. 1. Fabrication process of a miniaturized fluorescence detection chip: (A) a flow chat of the packaging process for a photodiode in PDMS (B) photograph of completed miniaturized fluorescence detection CE chip.

the channel [25,26]. Fig. 1B shows a completed miniaturized fluorescence detection chip, and Fig. 2 shows that the alignment of microfluidic channel and photodiode was successful and the thickness of PDMS interlayer was less than 20 μm . Although the smaller gap is better for the collection efficiency of photodiode, the gap smaller than 20 μm did not guarantee reliable bonding. Glass chips are also fabricated by traditional wet etching method and thermal bonding to compare the separation efficiency with PDMS microfluidic chip. Both the glass chip and PDMS chip were fixed by engineering plastic holder and a platinum wire was inserted into each reservoir as a contact for high voltage power supply.

2.3. Reagents and preparation of microchannel

All reagents were of analytical grade and solutions were purchased from Sigma–Aldrich (St. Louis, MO). They were

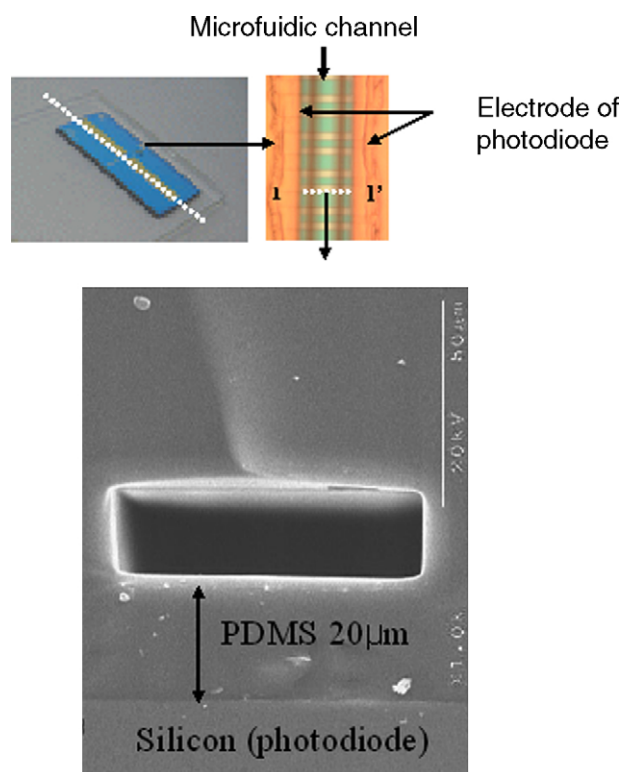


Fig. 2. Microscope images and a cross sectional SEM image of the miniaturized fluorescence detection chip. The width and depth of microfluidic chip are 70 μm and 12 μm respectively. The microchip is 25 mm wide and 50 mm long with a four-way injection, 27 mm-long separation channel and 8 mm-long sample loading channels.

prepared with distilled water, which was boiled prior to preparation of the entire set of standards and reagents to make it free from dissolved oxygen. A running buffer was a mixture of 1M NDSB (non-detergent sulfobetaine) and 1% tween 20 in 20 mM sodium phosphate of pH 7.4. PB (polybren) and DS (dextran sulfate) were used as cationic and anionic coating agent in PDMS chip. Fluorescein-labeled atrazine and anti-atrazine antibody solutions were diluted with running buffer.

The fluorescein-labeled atrazine was synthesized as previously described in [27]. Briefly, the carboxylic acid of atrazine was activated by incubating overnight with the pre-dissolved mixture of NHS (*N*-hydroxysuccinimide) and EDC (1-ethyl-3-(3-dimethylaminopropyl) carbodiimide hydrochloride). Fluorescein thiocarbonyl ethylenediamine was then added to the incubation mixture, and the conjugated product was purified by a preparative thin layer chromatography. A monoclonal antibody specific to the carboxylic derivative of atrazine conjugate to bovine serum albumin [28] was kindly provided by Dr. Myung Ja Choi (KIST, Korea).

Microfluidic channel and capillary of Beckman P/ACE2100 system were rinsed with 1M NaOH for 30 min and then deionized water for 20 min in order to clean the channel and to enhance the dissociation of the silanol groups [29]. PDMS chip was rinsed with 5% PB solution for 15 min to form the first cationic layer. After coating with 10% DS solution, the channel was rinsed for 15 min to form the second anionic layer, followed by the coating of 5% PB solution over the anionic layer for 20 min.

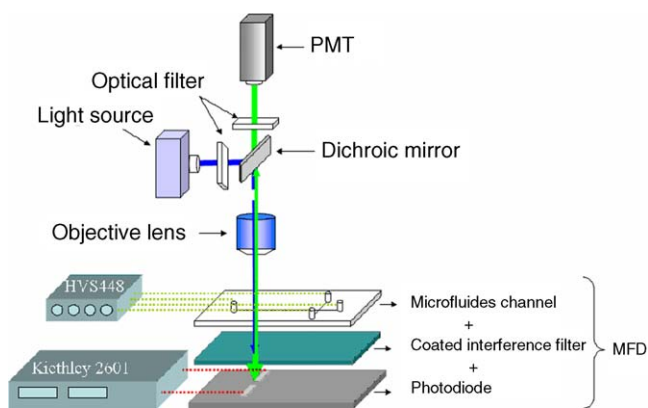


Fig. 3. Schematic of the experimental setup. The current of photodiode in microchip was recorded by a measurement system (Keithley 2601) and the fluorescence from the channel was also recorded by PMT through objective lens. Pinching and injection of sample were observed by fluorescence microscope and the electroosmotic flow was controlled by high voltage sequencer (LabSmith, HVS448).

These successive multiple ionic-polymer (SMIL) coating enables the PDMS chip to enhance the electroosmotic stability [30–33].

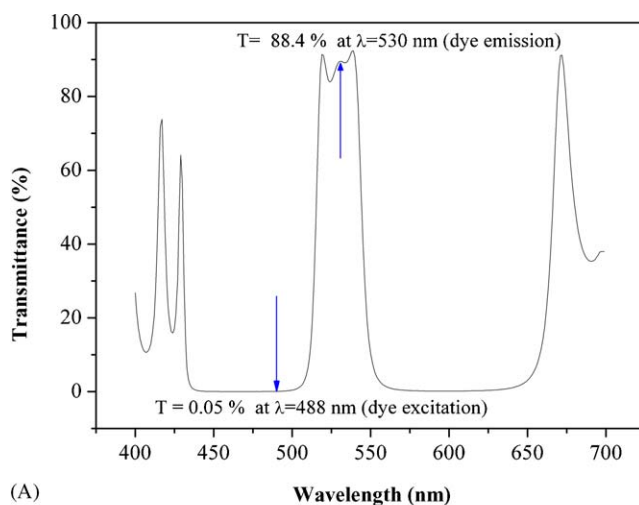
2.4. Measurement system

The current of photodiode in microchip was measured by a source and measurement system (Keithley 2601) and the fluorescence of channel was also recorded by PMT through microscope objective lens. Pinching and injection of fluorescein were observed by fluorescence microscope and the electroosmotic flow was controlled by high voltage sequencer (LabSmith, HVS448) as shown in Fig. 3. All instrumental control and data acquisition were operated by control program run by personal computer. Mercury lamp (Philips, 100 W) was used as a light source in fluorescence detection. The incident light from the lamp was filtered by optical filter (wavelength ~ 488 nm) and was focused on the microfluidic chip by objective lens. Also, commercial CE equipment was Beckman P/ACE2100 system with 27 cm-long uncoated fused silica capillary (Beckman) with the internal diameter of 50 μm .

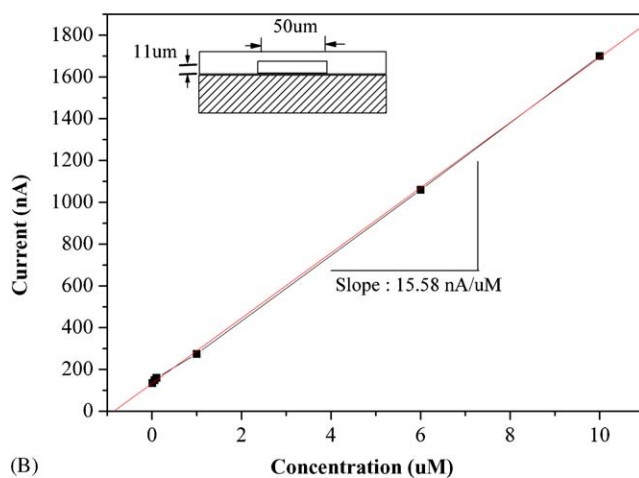
3. Results and discussion

3.1. Optical filter and the performance of detector

The interference filter deposited on the photodiode was used to filter the fluorescence light from the excitation beam. Atrazine was labeled with fluorescein in CE experiment, which has an absorption maximum at 488 nm and an emission maximum at 530 nm. Hence the filter was fabricated to block more than 99.95% of the excitation wavelength and to transmit more than 80% of the fluorescence at the range of 510–550 nm (Fig. 4A). The efficiency of filter is critical to the sensitivity of sensor because the background noise is largely dependent on the transmitted excitation light. Since the transmittance of 0.05% of incident light is relatively larger than the LIF system,



(A)



(B)

Fig. 4. Characteristics of photodiode, optical filter: (A) transmittance vs. wavelength at interference optical filter on the photodiode. The filter was fabricated to block more than 99.95% of the excitation light and to transmit more than 80% of the fluorescence in the range of 510–550 nm (B) Output currents of the photodiode vs. concentration with external laser source (2 mW). The slope of response was $15.58 \text{ nA}/\mu\text{M}^{-1}$ with the standard deviation of 32 pA. The limit of detection was at least 6 nM when the signal to noise ratio (SNR) is more than 3.

we needed to investigate the limit of detection of miniaturized detection system. The PDMS microfluidic channel, 50 μm wide and 11 μm deep, was filled with fluorescein and the current of photodiode was measured where the light source was laser of 2 mW power. The concentration of fluorescein was changed from 10 nM to 10 μM and the background signal was as large as 135 nA. The slope of linear response was $15.58 \text{ nA } \mu\text{M}^{-1}$ with the deviation of 32 pA. The limit of detection in the microchip was at least 6 nM when the signal to noise ratio (SNR) was more than 3. According to a standard of Environmental Protection Agency (EPA) in United States, the allowed maximum concentration of atrazine in drinking water is 0.003 mg L^{-1} , which is equivalent to 13.91 nM of atrazine. Since the experimental limit of detection seemed to just cover the EPA standard, the result implies that the miniaturized detection system is not enough to produce reliable and reproducible quantitative data because it is generally accepted that the limit of quantification is five times

of standard deviation, in which case 13.19 nM is close to the this value (about 10 nM).

3.2. CE immunoassay of atrazine in commercial CE system

Before we proceeded to CE immunoassay on PDMS chip, we needed to set-up the experimental conditions for the separation of atrazine and immunocomplex. Commercial CE system was used to optimize running buffer condition and the field strength. Injection interval was 1 s with 0.5 psi and the running buffer was 20 mM sodium phosphate buffer at pH 7.4 for separation. The applied voltage was 10.8 kV (400 V cm^{-1}) at 27 cm-long fused-silica capillary of 50 μm diameter. The sample was the mixture of fluorescein-labeled atrazine (Ag^*), anti-atrazine antibody (Ab), immunocomplex (Ab- Ag^*) and FITC in commercial CE system, where 50 nM FITC was inserted as an internal standard peak. The peaks of labeled-antigen and immunocomplex were normalized by maximum peak magnitude of FITC. After immunocomplex (Ab- Ag^*) peak was first observed, atrazine (Ag^*) and FITC peaks appeared in sequence owing to the charge to mass ratio (Fig. 5A). As the concentration of anti-atrazine increased, the peak of Ag^* was rapidly decayed while that of Ab- Ag^* was slowly increased. Less change of the peak of Ab- Ag^* came from the quenching effect that occurs when the antibody binds to atrazine. All peaks appeared in approximately 190 s and the calculated separation efficiency was 35,000 plates for the atrazine.

The concentration of antibody was changed from 37 to 730 nM to investigate the binding efficiency of anti-atrazine antibody, where the concentration of atrazine was fixed to 100 nM. From the repeated separation results, the concentration of immunocomplex was plotted as a function of that of antibody (Fig. 5B). The concentration of immunocomplex was saturated around 90 nM when the concentration of antibody was more than 300 nM. The curve fitting of the data shows that the dissociation constant (K_d) of reaction was about 37.5 nM.

3.3. CE immunoassay of atrazine in glass microfluidic chip

Based on the experiments of commercial CE system, we performed immunoassay of atrazine with microfluidic chip. The injection was implemented by electroosmotic flow and the sample was separated by capillary zone electrophoresis. Since the surface of PDMS microchip is not easy to control, we first set-up the bias conditions of injection and separation (Table 1) with glass microchip. Experimental set-up was shown in Fig. 6, where the location of reservoir and the electrodes of photodiode were depicted. When the glass chip was used in separation, the fluorescence was detected by PMT attached at the top of microscope.

Table 1
Bias condition of the capillary electrophoresis in microfluidic chip (*represents the electric field of separation)

Injection/separation	R (V)	L (V)	C (V)	W (V)
Glass (200 V cm^{-1})*	600/500	0/500	600/800	700/0
PDMS (200 V cm^{-1})*	-500/-400	0/-400	-500/-700	-600/0

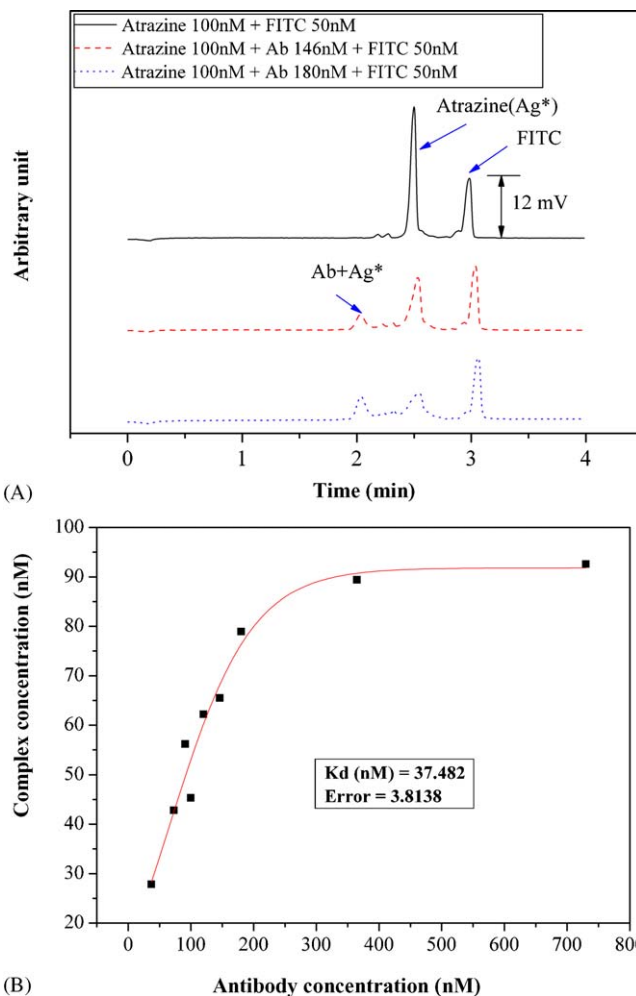


Fig. 5. Immunoassays in conventional capillary electrophoresis: (A) electropherogram of FITC-labeled atrazine and anti-atrazine. The peaks of labeled-antigen and immunocomplex were normalized by the peak height of FITC. (B) the concentration of immunocomplex as a function of antibody concentration. The curve fitting of the data shows that the dissociation constant (K_d) of reaction was about 37.5 nM.

The electropherogram obtained using glass chip coincided with that of commercial CE system (Fig. 7A), which implied that the CE immunoassay of atrazine in microfluidic channel was reproduced. The concentration of atrazine and FITC were 570 and

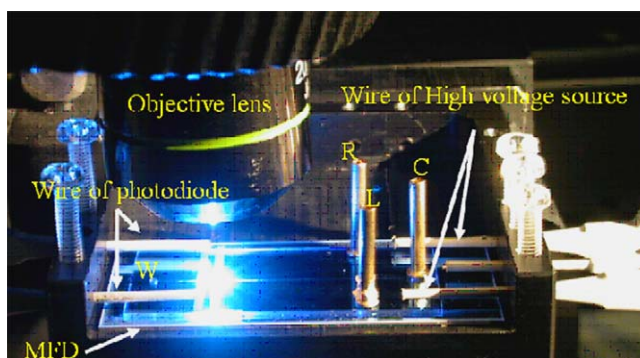


Fig. 6. Photograph of the experimental configuration. Reservoirs R, sample; L, sample waste; C, running buffer; D, buffer waste.

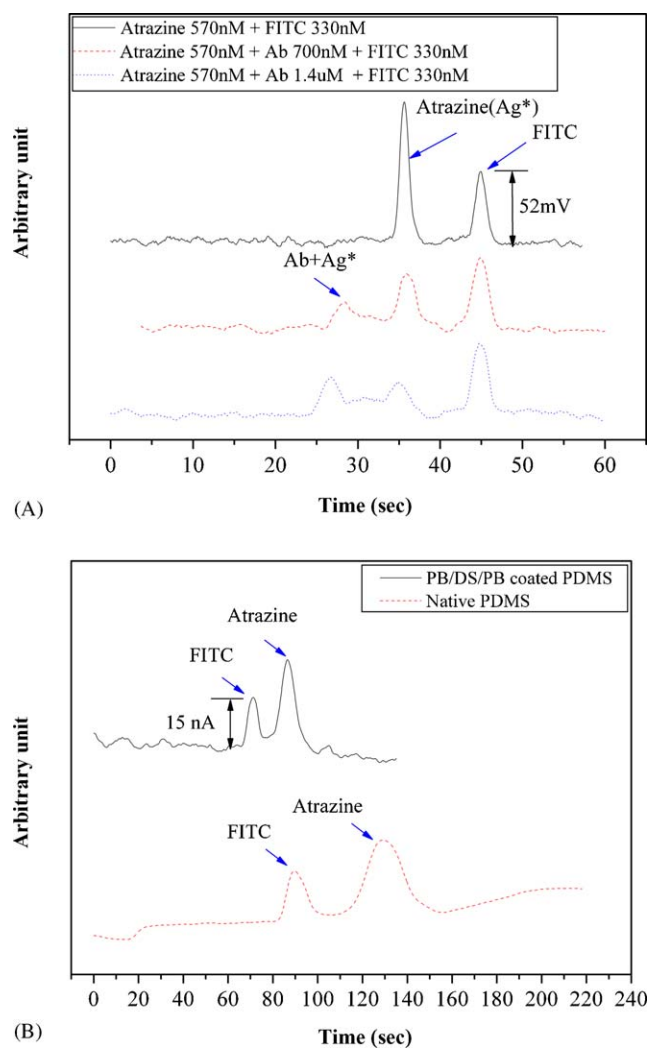


Fig. 7. Immunoassays in microfluidic chips: (A) electropherogram of FITC-labeled atrazine and anti-atrazine in a glass microfluidic chip. The peaks of labeled-antigen and immunocomplex were normalized by the peak height of FITC. (B) the electropherogram in a native PDMS and a PB/DS/PB-coated PDMS microfluidic channels. The sequence of peaks was reversed; the peak of FITC was first appeared, the peaks of Ag^* and Ab- Ag^* were followed sequentially.

330 nM, respectively. The concentration of reagents was higher than that in commercial CE system due to the short light path and small injection volume in microfluidic channel. The cross sectional area of capillary in commercial CE system was three times larger than that in microchip CE. The injection volume was related to the intensity of fluorescence and relevant to the limit of detection in CE immunoassay. The concentrations of antibody were 700 nM and 1.4 μ M and the peak of labeled-antigen were much decreased by the addition of antibody. Although the peak of immunocomplex was not as distinct as that of CE system, the separation time of in glass microchip was shorter owing to the small injection volume and the short length of fluidic channel. The applied electric field was 200 $V\ cm^{-1}$ and the highest applied voltage was 800 V. Despite low electric field, the separation efficiency was comparable to that of CE system due to the high heat conduction through the substrate of microchip. If we

used longer separation channel, separation efficiency could be improved. The experimental results in glass microchip verified that microchip CE is enough for the immunoassay of atrazine.

3.4. CE immunoassay of atrazine in PDMS microchip with integrated photodiode

Although glass microchip CE recapitulated the electropherogram of commercial CE system, it was not easy to integrate the photodiode near the microfluidic channel made of glass. The glass chip was not suitable for the integration of photodiode with microchip since the gap between the channel and photodiode is more than 500 μ m. If we attach the photodiode at the bottom of glass chip, the collection efficiency of fluorescence will be deteriorated since the fluorescence in channel spread out all directions. As the gap increases, the angle of light accepted by photodiode becomes smaller and the level of background noise increases.

PDMS is convenient to integrate photodiode on PDMS microfluidic channel since the bonding process between photodiode and microfluidic channel is of no difficulty. Therefore, we fabricated miniaturized fluorescence detection chip with PDMS and that was applied to the portable detection of atrazine using CE immunoassay. However the surface property of PDMS is apt to change with the environment and PDMS cannot sustain hydrophilicity after plasma oxidation. Electroosmotic mobility of native PDMS was not steadily stable and the flow by electrokinetic pumping was not always same. When the mixture of atrazine and antibody was separated in native PDMS microfluidic channel, the sequence of peaks was reversed. That is to say, after the peak of FITC was first appeared, the peaks of Ag^* and Ab- Ag^* were followed sequentially. It was caused by that the electrophoretic velocity of labeled particles were larger than that of electroosmotic flow due to the low electroosmotic mobility of PDMS surface. To compare the electroosmotic mobility of the glass channel and PDMS channel, we used current monitoring method. This follows Ohm's law in the channel when an electrolyte of different ionic strength fills the channel. The time required for the current to reach a steady state can be used to calculate the electroosmotic mobility. The measured electroosmotic mobility of glass and PDMS were about 4.4 and 2.3, respectively (Table 2), which were quite similar to those of previous report [34]. PDMS channel has approximately two times lower electroosmotic mobility and that affects the separation efficiency.

To stabilize the surface of PDMS, surface condition was modified by ionic polymer coating. We chose PB and DS as coating material and the final coating layer was cationic layer (PB), which reversed the direction of electroosmotic flow. Electropherogram of a native PDMS has larger width and longer

Table 2
Electro-Osmotic flow in a glass and a PDMS chips

	Applied voltage (V)	EOF ($\times 10^{-4}\ cm^2\ V^{-1}\ s^{-1}$)
Glass	500	4.2–4.6
PDMS	–500	2.1–2.5

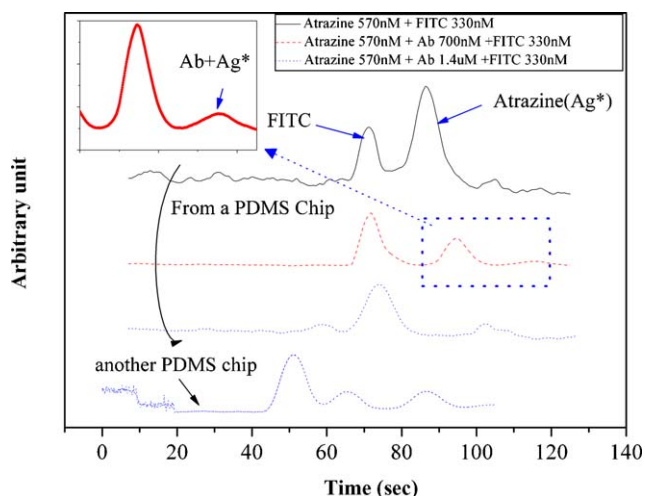


Fig. 8. Electropherogram of competitive immunoassay in PDMS microchip. The raw data of photodiode were processed with adjacent averaging process of 10 data points. The concentration of antibody was sequentially changed in the same PDMS chip and three upper electropherograms are plotted. The fourth plot was the electropherogram from another PDMS chip.

separation time than that of a PB/DS/PB-coated PDMS at the same bias condition (Fig. 7B). Furthermore, it is shown that the baseline of native PDMS was drifted because analyte slowly leaked out from the channel surface [33]. PB/DS/PB coating on PDMS channel was effective in reducing the time of migration and in improving the stability of separation.

With the coated-PDMS chip, we performed the separation of mixture of labeled-antigen and anti-atrazine antibody. Fig. 8 shows the electropherograms of CE immuno-reaction in PDMS microchip, where the raw data of photodiode were processed with adjacent averaging process of 10 data points. The concentration of antibody was sequentially changed in the same PDMS chip and three electropherograms are plotted from top to bottom. Compared with the result of glass, the peak of immunocomplex ($Ab-Ag^*$) was weakly appeared but the decrease of Ag^* peak was clearly observed with the increase of the concentration of antibody. Despite the coating of ionic polymer, it is observed that the second and the third separations were delayed by about 10 s. To get rid of the stacking effect, PDMS chip was replaced by new fresh chip. $Ab-Ag^*$ peak from the fresh PDMS chip was observed in fourth plot but the migration time was quite shorter than that of previous PDMS chip.

Although multi-layer coating procedure increased the stability of performance, the reproducibility of coated PDMS was not enough to obtain fixed retention time with every chip due to the extrinsic conditions. Main factor affecting the surface property of PDMS is the stability of hydroxyl group layer after oxygen plasma treatment, since the electrostatic binding of ionic polymer depends on the previous state of the pre-treated wall. These extrinsic factors could be removed by the management of process environment and coating procedure.

The results from Figs. 7 and 8 represent that separation of atrazine could be carried out in microfluidic channel and the immuno-reaction of atrazine can be detected by embedded photo detector, although the detection limit was far higher than the

commercial CE system. All peaks of electropherograms with glass microchip were resolved in approximately 50 s with separation efficiency of 4800–6400 plates for the atrazine. With PDMS chip, the total separation time increased to 110 s and separation efficiencies ranged from 3000 to 5200 due to the low electroosmotic flow. However, despite the lower electroosmotic flow and smaller plate numbers, acceptable separations of the atrazine were recapitulated on the PDMS channel with the integrated photodiode.

4. Conclusion

Low cost silicon-based PIN photodiode with interference filter was packaged in PDMS microfluidic chip and the miniaturized fluorescence detection chip was applied to analyze the atrazine using CE immunoassay. The fluorescence of separated atrazine was effectively detected with the embedded photodiode and the capillary electrophoresis in microfluidic chip was performed in short time. This work proved that the portable detection of CE immunoassay of atrazine is feasible because the hardware for data acquisition and electrokinetic pumping could be miniaturized. Besides, tens of small molecules could be detected simultaneously with the array of photodiodes with the power of multiplexed CE immunoassay.

However, the low sensitivity in separation still hinders the realization of portable detection of small molecules, even though the detection limit of photodiode was almost close to the required specification of EPA. Fortunately, there are lots of methods to enhance the analytical sensitivity such as the improvement of filter efficiency, the stable coating of PDMS, and the additional sample pre-concentration in microfluidic chip. Furthermore, other substrate material for microfluidic chip could be considered because PDMS is inappropriate for mass production and long term storage. The candidates would be injection-molded plastic chip or polymer film chip. Conclusively miniaturized fluorescence detection chip can be applied to CE immunoassay of small molecule if the surface conditioning process is improved or sample pre-treatment is added since it has merits of low cost, small size and simple fabrication.

References

- [1] A. Manz, Y. Miyahara, J. Miura, Y. Watanabe, H. Miyagi, K. Sato, *Sens. Actuators B* (1990) 249.
- [2] K.B. Mogensen, N.J. Petersen, J. Hübner, J.P. Kutter, *Electrophoresis* 22 (2001) 3930.
- [3] M. Kato, K. Sakai-Kato, H.M. Jin, K. Kubota, H. Miyano, T. Toyooka, M.T. Dulay, R.N. Zare, *Anal. Chem.* 76 (2004) 1896.
- [4] Y. Pico, R. Rodriguez, J. Manes, *Trends Anal. Chem.* 22 (2003) 133.
- [5] G. Dinelli, A. Vicari, P. Catizone, *J. Chromatogr. A* 733 (1996) 337.
- [6] Z. El Rassi, *Electrophoresis* 18 (1997) 2465.
- [7] A.K. Malik, W. Faubel, *Crit. Rev. Anal. Chem.* 31 (2001) 223.
- [8] K.B. Mogensen, H. Klank, J.P. Kutter, *Electrophoresis* 25 (2004) 3498.
- [9] M.E. Johnson, J.P. Landers, *Electrophoresis* 25 (2004) 3513.
- [10] V. Namasivayam, R. Lin, B. Johnson, S. Brahmasandra, Z. Razzacki, D.T. Burke, M.A. Burns, *J. Micromech. Microeng.* 14 (2004) 81.
- [11] A.M. Jorgensen, K.B. Mogensen, J.P. Kutter, O. Geschke, *Sens. Actuators B* 90 (2003) 15.
- [12] J.B. Edel, N.P. Beard, O. Hofmann, J.C. deMello, D.D.C. Bradley, A.J. deMello, *Lab. Chip* 4 (2004) 136.

- [13] T. Yamamoto, T. Nojima, T. Fujii, *Lab. Chip* 2 (2002) 197.
- [14] P.F. Wagler, U. Tangen, T. Maeke, H.P. Mathis, J.S. McCaskill, *Smart Mater. Struct.* 12 (2003) 757.
- [15] J.C. McDonald, D.C. Duffy, J.R. Anderson, D.T. Chiu, H. Wu, O.J.A. Shueller, G.M. Whitesides, *Electrophoresis* 21 (2000) 27.
- [16] S. Chamberlain, *IEEE Trans. Electron Devices* 34 (1979) 7228.
- [17] M.L. Chabinyc, D.T. Chiu, J.C. McDonald, A.D. Stroock, J.F. Christian, A.M. Karger, G.M. Whitesides, *Anal. Chem.* 73 (2001) 4491.
- [18] P. Krulevitch, W. Bennett, J. Hamilton, M. Maghribi, K. Rose, *Biomed. Microdev.* 4 (2002) 301.
- [19] J.B. Edel, N.P. Beard, O. Hofmann, J.C. deMello, D.D.C. Bradleyb, A.J. deMello, *Lab. Chip* 4 (2004) 136.
- [20] J. Chen, W. Wang, J. Fang, K. Varahramyan, *J. Micromech. Microeng.* 14 (2004) 675.
- [21] E. Thrush, O. Levi, W. Ha, G. Carey, L.J. Cook, J. Deich, S.J. Smith, W.E. Moerner, J.S. Harris Jr., *J. Quantum Electron.* 40 (2004) 491.
- [22] M.L. Adams, M. Enzelberger, S. Quake, A. Scherer, *J. Sens. Actuators A* 104 (2003) 25.
- [23] M. Kyomasu, *IEEE Trans. Electron Devices* 42 (1995) 1093.
- [24] C.-H. Lin, G.-B. Lee, Y.-H. Lin, G.-L. Chang, *J. Micromech. Microeng.* 11 (2001) 726.
- [25] S. Satyanarayana, R.N. Karnik, A. Majumdar, *J. Microelectromech. Syst.* 14 (2005) 392.
- [26] H. Katayama, Y. Ishihama, N. Asakawa, *Anal. Chem.* 70 (1998) 5272.
- [27] M.J. Choi, J.R. Lee, S.A. Eremin, *Food Agri. Immunol.* 14 (2002) 107.
- [28] M.J. Choi, Y. Jo, J. Choi, C. Kang, C.T. Han, *J. Immunoassay* 20 (1999) 57.
- [29] G.J.M. Bruin, R. Huisden, J.C. Kraak, H.J. Poppe, *J. Chromatogr.* 480 (1989) 339.
- [30] B.J. Herren, S.G. Shafer, S.V. Alstine, J.M. Harris, R.S. Snyder, *J. Colloid Interface Sci.* 115 (1987) 46.
- [31] D. Schmalzing, C.A. Piggee, F. Foret, E. Carriho, B.L. Karger, *J. Chromatogr. A* 480 (1993) 149.
- [32] X. Huang, C. Horvath, *J. Chromatogr. A* 788 (1997) 155.
- [33] N.A. Lacher, N.F. de Rooij, E. Verpoorte, S.M. Lunte, *J. Chromatogr. A* 1004 (2003) 225.
- [34] X. Ren, M. Bachman, C. Sims, G.P. Li, N. Allbritton, *J. Chromatogr. B* 782 (2001) 117.